Scaling of the transition to parametrically driven surface waves in highly dissipative systems

O. Lioubashevski,[1] J. Fineberg,[1] and L. S. Tuckerman[2]
[1]*The Racah Institute of Physics, The Hebrew University of Jerusalem, Jerusalem 91904, Israel*
[2]*Laboratoire d'Informatique pour la Mécanique et les Sciences de l'Ingénieur, Boîte Postale 133, 91403 Orsay Cedex, France*

(Received 23 May 1996; revised manuscript received 7 November 1996)

We present an experimental study of the onset of the Faraday instability in highly dissipative fluids. In this regime of high viscosity and shallow fluid depth, we find that the critical acceleration for the transition to parametrically excited surface waves scales as a function of two dimensionless parameters corresponding to the ratios of the critical driving amplitude height and viscous boundary layer depth to the fluid depth. This scaling, which exists over a wide range of fluid parameters, identifies the proper characteristic scales and indicates that a Rayleigh-Taylor type mechanism drives the instability in this regime. [S1063-651X(97)51004-X]

PACS number(s): 47.52.+j, 47.35.+i, 47.54.+r, 47.20.Gv

The Faraday instability, which generates parametrically driven surface waves, is one of a number of well-known pattern-forming systems. It occurs when a featureless layer of fluid, subjected to uniform, externally imposed oscillations in the vertical (parallel to gravity) direction, becomes unstable to the spontaneous appearance of surface waves. The acceleration a of the fluid layer can be viewed as the system's control parameter. The waves appear at a critical value of the layer acceleration, a_c, and oscillate at half of the external driving frequency. The system is further characterized by the quantities ω, h, ν, ρ, L, and σ defined as the externally imposed angular frequency, depth of the fluid layer, kinematic viscosity, fluid density, lateral size of the system, and surface tension, respectively.

Most previous experiments [1] in this system were performed in the low ν, large h limit where the linear dynamics of the system are described by the Mathieu equation [2] with dissipation, which governs the instability threshold, introduced phenomenologically [3,4]. In this regime, careful experiments by Christiansen *et al.* [5] showed the instability threshold to scale as $a_c = 2\nu\omega k/\tanh(hk)$ when corrections [4] to the dissipation due to the moving contact line between the fluid and the lateral walls bounding the experimental cell are taken into account.

Recent experiments have shown the utility of working in a regime of high fluid viscosity and relatively shallow fluid layers [6–8]. In this region of phase space, external disturbances to the system are effectively damped out and the strong quantization of the unstable wave numbers in the system, enforced by the lateral boundaries, is relaxed. Thus, the effective number of modes that can be excited in the system near onset is increased [6,7]. In this region, Kumar and Tuckerman [9] showed that a_c, calculated numerically from the Navier-Stokes equation, deviates significantly from the threshold values predicted in the low ν, high h limit. These and later calculations in this regime agree well with measurements of a_c that were performed for a number of different values of h and ν in systems driven at both one [6,7] and two [10,11] frequencies.

Although numerical agreement between the calculations in [9] and experiment is established, once we are far from the low ν, high h limit in parameter space, the proper scaling behavior of a_c is unknown. There is some question as to whether a well-defined, scaling relation for a_c exists at all in the case of the Faraday instability. The eight quantities a, ω, ν, ρ, σ, h, L, along with the gravitational acceleration g can be combined in *five* dimensionless parameters. There is, of course, an infinite number of ways to choose these five parameters. The optimal choice is that which effectively reduces the number of parameters: that is, the dependence on some of the parameters is shown to be negligible in the range of interest.

In this paper we demonstrate that simple scaling of the critical acceleration indeed occurs in a surprisingly wide range of experimental parameters and the dominant dimensionless parameters in the high ν, low h regime are identified. As a result, the dimension of parameter space is effectively reduced from 5 to a more tractable 2. The form of these parameters suggests that, in this regime, a mechanism akin to the Rayleigh-Taylor instability may drive the instability.

Our experimental apparatus was previously described in [8]. Experiments were performed in a 144.0 mm diameter circular cell where the fluid is supported by an aluminum plate, polished to a mirror surface and flat to 1 μm. The cell's lateral boundaries, made of Delrin, were sloped at a 20° angle to reduce meniscus formation on the fluid surface. The fluid depth varied between 1.0 and 5.0 mm. Fluids used were glycerol-water mixtures and the hydrocarbon flushing fluids [12], TKO-FF (described at length in [8]) and TKO-77. The fluid temperature was regulated to within 0.01 °C. In the latter fluids σ and ν were varied between 29.6 and 31.0 dyn/cm and 4.7 to 0.25 S (1 S=1 cm/s) respectively as the temperature was varied over a 20–45 °C range.

The cell was mounted on a mechanical shaker providing vertical acceleration from 0 to 30g over a frequency range of 20–80 Hz. The acceleration, monitored by a calibrated accelerometer, was regulated to within 0.01g. To determine the instability onset, the system was visualized from above by shadowgraph with stroboscopic illumination. Two effects contribute to the experimental error in determining a_c. The first of these is due to experimental uncertainties in h (0.3–1.5%), ν (<3%), and the precision of a_c measurements (<0.5%). The second contribution to the error involves un-

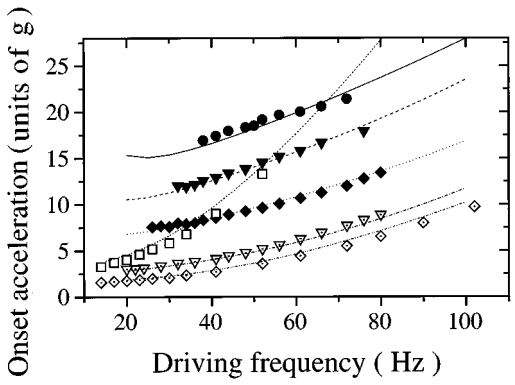

FIG. 1. Typical instability threshold measurements for $h=0.13$ cm, $\nu=0.8$ S (●), $h=0.15$ cm, $\nu=0.8$ S (▼), $h=0.15$ cm, $\nu=0.58$ S (◆), $h=0.21$ cm, $\nu=0.48$ S (△), $h=0.25$ cm, $\nu=0.41$ S, (◇), $h=0.51$ cm, $\nu=2.53$ S (□), The lines represent the calculated values for the threshold.

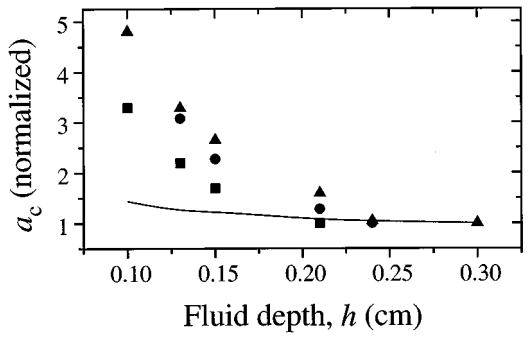

FIG. 2. The instability threshold a_c as a function of h for $\omega/(2\pi)=41$ Hz and $\nu=0.58$ S, (■), $\nu=0.8$ S (●), and $\nu=0.48$ S (▲). To facilitate comparison, a_c in each plot was normalized by the smallest measured threshold value in each data set. For comparison, we include (solid line) the predictions for large h low ν regime.

certainty (~5%) in the absolute value of a_c resulting from slight inhomogeneities in the apparatus leveling. Although, for given conditions, the value of a_c is entirely reproducible, a 0.1 mrad tilt of the apparatus, at small values of h, can induce a shift of a few percent, in absolute value. Additional shifts [7] of a few percent in a_c can occur due to lateral quantization of the wave number λ at very low values of ω (large λ).

Fluid patterns observed in the near vicinity of a_c throughout nearly the entire measured ν,h,ω parameter space are subharmonic, spatially localized states (''confined states'' as observed in [8]) with no observed hysteresis in the transition [13]. Globally distributed patterns were only observed when λ was *within* an order of magnitude of the cell diameter and mode quantization was enforced by the lateral boundaries of the system.

In Fig. 1 we present typical plots of both measured and calculated values of a_c as a function of ω for different values of h and ν. As the figure shows, for a given excitation frequency, a_c can vary by over an order of magnitude as the fluid height and viscosity are varied. In looking for scaling behavior in the system, our first task is to identify the characteristic length and time scales that lead to dissipation in the system. In Fig. 2 we plot the change in a_c as a function of h for a fixed value of ω and different values of ν. The strong dependence of a_c on h contrasts sharply with the instability threshold observed in the low ν, large h regime (line in the figure) where λ is considered to be the dissipative length scale. In the high ν, low h regime, the dependence of a_c on λ is negligible in contrast to its strong h dependence until approximately $\lambda/h<4$. This suggests that, in this regime, the dominant dissipative scale in the system is h.

We use this scale to determine the proper dimensionless parameters in this regime. Non-dimensionalizing length by h, time by ω^{-1}, mass by ρh^3, and defining the viscous boundary layer height as $\delta\equiv(\nu/\omega)^{1/2}$, we obtain the five dimensionless quantities $a/(h\omega^2),\nu/(\omega h^2)\equiv(\delta/h)^2$, $\sigma/(\rho\omega^2h^3)$, L/h, and $g/(h\omega^2)$. In Fig. 3 we plot the scaled acceleration threshold, $a_c/(h\omega^2)$, as a function of the parameter $(\delta/h)^2$, which characterizes the dissipation in the system. Although the values of a_c in the figure typically span over an order of magnitude for a given value of δ/h, the data when scaled, largely collapse onto a single curve. The data in Fig. 3 also cover a wide range of the other dimensionless parameters. In particular, $0.001<\sigma/(\rho\omega^2h^3)<0.7$, $20<L/h<140$, and $0.01<g/(h\omega^2)<0.6$.

A closer look at some experimental data sets, however, reveals systematic deviations from scaling. Guided by these, we have extended our data by performing numerical calculations using the Kumar-Tuckerman algorithm [9] (lines in Fig. 3) for parameter combinations chosen to display a more marked deviation from the scaling suggested by the figure.

The deviations from scaling occur in precisely the region $(\lambda/h)^2\gg1$, where we would most expect the scaling to hold for the following reason. The parameter δ/h governs the dissipation in the system. Our choice of h as the characteristic length in the system is equivalent to stating that the dominant dissipative mechanism in the system is the shear between the fluid flow and the bottom plate. This dissipation is balanced against the parameter $a_c/(h\omega^2)$, or the driving term, which, when large enough, leads to instability of the fluid surface. In

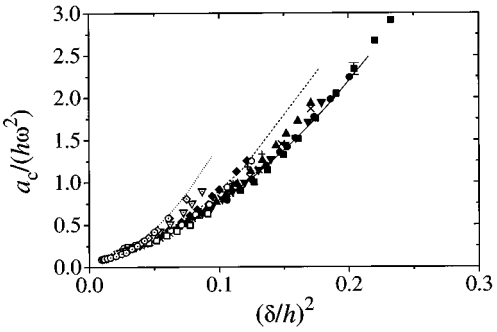

FIG. 3. Scaling of reduced acceleration threshold, $a_c/(h\omega^2)$, as a function of the dissipation parameter $(\delta/h)^2$. Experimental data (h in cm, ν in S): $h=0.1$, $\nu=0.58$ (■), $h=0.13$, $\nu=0.58$ (▲), h=0.13, $\nu=0.8$ (●), $h=0.15$, $\nu=0.8$ (▼), $h=0.15$, $\nu=0.48$ (◆), $h=0.21$, $\nu=0.8$ (+), $h=0.21$, $\nu=1.23$ (x), $h=0.24$, $\nu=0.8$(*) $h=0.3$, $\nu=1.23$(○), $h=0.51$, $\nu=2.53$ (□), $h=0.21$, $\nu=0.48$ (△), $h=0.25$, $\nu=0.41$ (◇), $h=0.3$, $\nu=0.48$ (⊙). Numerical data: $h=0.13$, $\nu=0.81$, (dot-dashed line) $h=0.15$, $\nu=0.50$, (dashed line) $h=0.13$, $\nu=0.20$ (dotted line). Note the systematic deviations from scaling.

the low ν, high h regime, $\delta/h \ll 1$ and the major mechanism for dissipation in the fluid bulk would instead be the shear over a pattern wavelength. Thus, when h is large, λ is the characteristic scale for dissipation, and, balancing the dissipative term with the driving recovers the scaling $a_c \approx \nu\omega k$. We would therefore expect the scaling behavior indicated by Fig. 3 to best hold in the limit where $(\lambda/h)^2 \gg 1$, which is realized over most of our experimental range ($1.5 > \lambda > 0.5$ cm, $0.5 > h > 0.1$ cm).

Since the thresholds, calculated for a laterally infinite system, agree well with the measured values, the source of the deviations cannot be the dissipation at the lateral boundaries observed by Christiansen *et al.* [5]. Moreover, we find that the scaled surface tension $\sigma/(\rho\omega^2 h^3)$ and aspect ratio L/h have a negligible effect on $a_c/(h\omega^2)$. [There was no observable change in $a_c/(h\omega^2)$ as either parameter was varied by about a factor of 5, while keeping δ/h fixed.] This leads us to consider the relevance of the remaining parameter, $g/(h\omega^2)$.

In order to better understand the dependence on $g/(h\omega^2)$, we consider the underlying equations governing the behavior of our system. These are the externally forced Navier-Stokes (NS) equation in the comoving reference frame and the boundary condition at the free fluid surface, which balances the normal stress with the Laplace pressure caused by the distorted surface. Nondimensionalizing length by h, time by ω^{-1}, and mass by ρh^3, these equations are

$$\partial_\tau \mathbf{v} + (\mathbf{v}\cdot\boldsymbol{\nabla})\mathbf{v} = -\nabla P + \left(\frac{\delta}{h}\right)^2 \nabla^2 \mathbf{v} + \frac{a}{h\omega^2}\left(\sin(\tau) - \frac{g}{a}\right) e_z \tag{1}$$

and

$$P = 2\left(\frac{\delta}{h}\right)^2 \partial_z w + \left(\frac{\sigma}{\rho h^3 \omega^2}\right)(\partial_x{}^2 + \partial_y{}^2)\zeta, \tag{2}$$

where the dimensionless quantities τ, $\mathbf{v}$, w, P, ζ, and e_z are, respectively, time, velocity, vertical velocity, pressure, height of the fluid, and the unit vector normal to the surface (the pressure above the layer is defined to be 0). We will not state explicitly the remaining boundary conditions, except to mention that they introduce the quantity L/h. (More details can be found in, e.g., [9].) As expected, we recover the five nondimensional parameters previously listed.

We now propose a description of the Faraday instability in this regime as a periodically driven version of the Rayleigh-Taylor instability. The Rayleigh-Taylor (RT) instability [14] occurs at the interface of two fluids when the denser fluid is forced into the lighter one. The initially planar interface then becomes unstable to a wide band of wave numbers. In our experiment, upon upward (against the direction of gravity) acceleration, the fluid layer is susceptible to this type of instability as it is forced into the layer of air above it. Due to the large width of the unstable band of wave numbers allowed by the RT instability, the selected wave number will still be determined by the forcing frequency via the fluid's dispersion relation. If the RT effect is dominant, we should take the full driving term, $a(\sin\tau - g/a)/(h\omega^2)$, into account when deriving the proper scaling. We do this by defining the parameter, $a(2/\pi - g/a)/(h\omega^2)$, which characterizes the mean *upward* acceleration over an excitation period.

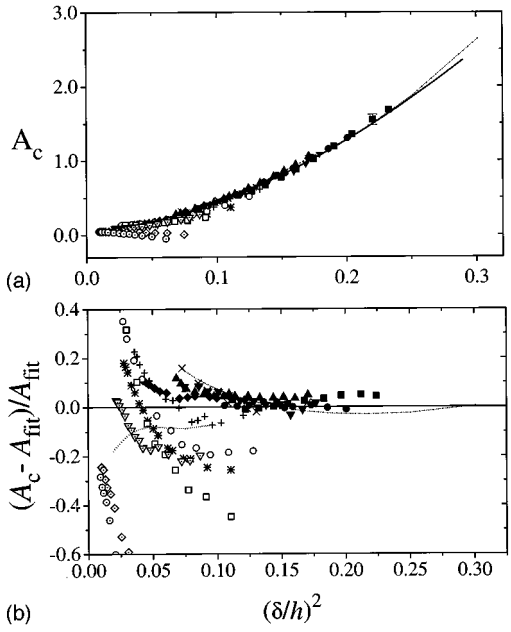

FIG. 4. (a) The scaled acceleration threshold, $A_c \equiv a_c(2/\pi - g/a_c)/(h\omega^2)$, with net upward acceleration taken into account. Note the following data sets where $a_c < 2 - 3g$: $h = 0.25$ cm, $\nu = 0.41$ S ($\diamond$), and $h = 0.3$ cm, $\nu = 0.48$ S, ($\odot$). The solid line, $A_{fit} = 0.059 + 21.46(\delta/h)^{3.54}$ is a fit to the data. Representative error bars are shown. (b) A high resolution plot of the relative deviations from scaling behavior, $(A_c - A_{fit})/A_{fit}$. The data and symbols used are as described in Fig. 3.

In Fig. 4 we replot the threshold data presented in Fig. 3 after rescaling the critical acceleration using $a_c(2/\pi - g/a_c)/(h\omega^2)$. The data collapse in the figure is markedly better. As a_c approaches g, the RT type mechanism for instability can no longer dominate and the scaling breaks down. Two data sets where this occurs are presented in the figure for $\nu = -0.46$ and 0.52 S with fluid depths of 0.25 and 0.3 mm, respectively. Empirically, we find that for $a_c > 2 - 3g$, the scaling works well.

A high resolution plot is presented in Fig. 4(b) where we subtract the measured data from the fit: $a_c(2/\pi - g/a_c)/(h\omega^2) = 0.059 + 21.4(\delta/h)^{3.54}$. For values of a_c where the RT type instability is relevant, there is little systematic deviation of the experimental data from the scaling function with the spread in the data falling within experimental error for $\delta/h > 0.1$. As in Fig. 4(a), large deviations from scaling are only seen for data where g/a_c approaches $2/\pi$. Surprisingly, the scaling holds even in data sets for which $\lambda \sim 2h$, where we might expect the shear (and hence the dissipation) over the horizontal scale of a pattern wavelength to be comparable with the shear between the fluid and cell bottom.

In conclusion, we have presented evidence for scaling behavior of the transition to parametrically driven surface waves over a wide range of experimental parameters in the regime of highly dissipative fluids. This scaling is derived by using the fluid height and driving period as the characteristic length and time scales. Of the dimensionless parameters se-

lected, the nondimensional surface tension $\sigma/(\rho\omega^2 h^3)$, and aspect ratio L/h have little effect on the transition; this justifies *a posteriori* the choices made in nondimensionalizing. We find that two parameters, $a_c(2/\pi - g/a_c)/(h\omega^2)$ and $(\delta/h)^2$, entirely govern the scaling of the transition in this regime. The first of these suggests that the instability, in this range of parameter space, is governed by a Rayleigh-Taylor type mechanism. The second parameter, $(\delta/h)^2$, was previously shown to govern the transition from localized patterns to highly localized propagating solitary states [8]. Understanding both the dominant scales and proper scaling of the system leads to a large reduction in the effective dimension of the parameter space and should facilitate the development of a theoretical description of both these states and other interesting nonlinear phenomena [6,8,15] recently observed in this regime.

The authors wish to acknowledge the support of the Wolfson Family Charitable Trust (Grant No. 43/93-2). We also thank B. Meerson, U. Alon, and H. Arbell for stimulating conversations and invaluable advice.

[1] See, e.g., N. B. Tufillaro, R. Ramshankar, and J. P. Gollub, Phys. Rev. Lett. **62**, 422 (1989); S. Ciliberto, S. Douady, and S. Fauve, Europhys. Lett. **15**, 23 (1991); A. B. Ezerskii, P. I. Korotin, and M. I. Rabinovich, Zh. Eksp. Teor. Fiz. **41**, 129 (1985), [Sov. Phys. JETP **41**, 157 (1986)]; E. Bosch and W. van der Water, Phys. Rev. Lett. **70**, 3420 (1993).

[2] T. B. Benjamin and F. Ursell, Proc. R. Soc. London, Ser. A **225**, 505 (1954).

[3] L. D. Landau and E. M. Lifshitz, *Fluid Mechanics* (Pergamon, New York, 1982).

[4] S. T. Milner, J. Fluid Mech. **225**, 81 (1991).

[5] B. Christiansen, P. Alstrom, and M. T. Levinsen, J. Fluid Mech. **291**, 323 (1995).

[6] W. S. Edwards and S. Fauve, Phys. Rev. E **47**, 788 (1993); J. Fluid Mech. **278**, 123 (1994).

[7] J. Bechhoefer, V. Ego, S. Manneville, and B. Johnson, J. Fluid Mech. **288**, 325 (1995).

[8] O. Lioubashevski, H. Arbell, and J. Fineberg, Phys. Rev. Lett. **76**, 3959 (1996).

[9] K. Kumar and L. S. Tuckerman, J. Fluid Mech. **279**, 49 (1994).

[10] J. Beyer and R. Friedrich, Phys. Rev. E **51**, 1162 (1995).

[11] T. Besson, W. S. Edwards, and L. S. Tuckerman, Phys. Rev. E **54**, 507 (1996).

[12] Obtained from the Kurt J. Lesker company.

[13] We can make no blanket statement regarding the existence of hysteresis throughout the entire parameter space. Within the 1% resolution in a_c of *typical* measurements no hysteresis was observed. A number of 0.1% resolution measurements were also performed, which also revealed no hysteretic behavior.

[14] M. S. Plesset and C. G. Whipple, Phys. Fluids **17**, 1 (1974).

[15] L. Daudet, V. Ego, S. Manneville, and J. Bechhoefer, Europhys. Lett. **32**, 313 (1995); A. Kudrolli and J. P. Gollub, Phys. Rev. E **54**, 1052 (1996).